

RESEARCH ARTICLE



Huoxue Qianyang Qutan recipe attenuates cardiac fibrosis by inhibiting the NLRP3 inflammasome signalling pathway in obese hypertensive rats

Bo Lu^{a*}, Jun Xie^{a,b*}, Deyu Fu^a, Xiaozhe Chen^{a,b}, Mingyi Zhao^{a,b}, Mingtai Gui^a, Lei Yao^a, Xunjie Zhou^a and Jianhua Li^a

^aDepartment of Cardiology, Yueyang Hospital of Integrated Traditional Chinese and Western Medicine, Shanghai University of Traditional Chinese Medicine, Shanghai, China; ^bShanghai University of Traditional Chinese Medicine, Shanghai, China

ABSTRACT

Context: HuoXue QianYang QuTan Recipe (HQQR) is used to manage hypertension and cardiac remodeling, but the mechanism is elusive.

Objective: To determine the mechanism of HQQR on obesity hypertension (OBH)-related myocardial fibrosis.

Materials and methods: OBH models were prepared using spontaneously hypertensive rats (SHRs) and divided ($n=6$) into saline, low-dose (19.35 g/kg/d) HQQR, high-dose (38.7 g/kg/d) HQQR, and valsartan (30 mg/kg/d) groups for 10 weeks. Systolic blood pressure (SBP), and Lee's index were measured. Heart tissues were examined by histology. HQQR's effects were examined on cardiac fibroblasts (CFs) stimulated with angiotensin II and treated with HQQR, a caspase-1 inhibitor, siNLRP3, and oeNLRP3.

Results: HQQR(H) reduced SBP (201.67 ± 21.00 vs. 169.00 ± 10.00), Lee's index (321.50 ± 3.87 vs. 314.58 ± 3.88), and left ventricle mass index (3.26 ± 0.27 vs. 2.71 ± 0.12) *in vivo*. HQQR reduced percentage of fibrosis area (18.99 ± 3.90 vs. 13.37 ± 3.39), IL-1 β (10.07 ± 1.16 vs. 5.35 ± 1.29), and inhibited activation of NLRP3/caspase-1/IL-1 β pathway. HQQR also inhibiting the proliferation (1.09 ± 0.02 vs. 0.84 ± 0.01), fibroblast to myofibroblast transition (14.74 ± 3.39 vs. 3.97 ± 0.53), and collagen deposition (Col I; 0.50 ± 0.02 vs. 0.27 ± 0.05 and Col III; 0.48 ± 0.21 vs. 0.26 ± 0.11) with different concentrations selected based on IC₅₀ *in vitro* (all $p < 0.05$). NLRP3 interference further confirmed HQQR inhibiting NLRP3 inflammasome signalling.

Conclusion: HQQR blunted cardiac fibrosis development in OBH and suppressed CFs proliferation by directly interfering with the NLRP3/caspase-1/IL-1 β pathway.

ARTICLE HISTORY

Received 26 April 2021

Revised 22 June 2021

Accepted 5 July 2021

KEYWORDS

Obesity; hypertension; traditional Chinese medicine; myocardial fibrosis; inflammation



Introduction

The worldwide prevalence of obesity is around 10.8 and 14.9% in men and women (Non-Communicable Disease Risk Factor [NCDRF] 2016; Afshin et al. 2017), and its prevalence is projected to increase substantially (Blucher 2019). Obesity is associated with hypertension and cardiovascular diseases (Chooi et al. 2019). Obese individuals have a 3.5-time higher risk of hypertension than non-obese (Marczak et al. 2018; Chooi et al. 2019). In addition, about (60–70%) of patients with hypertension are obese (i.e., obesity hypertension [OBH]) (Zhang et al. 2019). OBH is a hemodynamic volume-loading disease that can significantly increase the occurrence of target organ damage, such as myocardial remodelling (Global Burden of Diseases, Injuries, and Risk Factors Study [GRF] 2020). Increased cardiac output is associated with an increase in lean and central fat masses. Increased stroke work is associated with volume overload and an offset of peripheral resistance (Aurigemma et al. 2013). Still, regardless of the arterial stress level, the left ventricle can continually adapt to the blood volume expansion related to obesity through creating eccentric hypertrophy (Susic and Varagic 2017). Cardiac fibrosis

is due to any injury to the heart, including myocardial infarction and cardiac remodelling. It is characterized by collagen deposition within the heart, leading to adverse outcomes, such as heart failure, arrhythmia, and unexpected cardiac death (Frangogiannis 2019; Hinderer and Schenke-Layland 2019). Despite progress in treatment options, the morbidity and mortality rates associated with cardiac remodelling/dysfunction are high (Hinderer and Schenke-Layland 2019).

Traditional Chinese medicine (TCM) could be effective in treating myocardial fibrosis. Indeed, Huoxue Qianyang Qutan Recipe (HQQR) is a TCM compound that has been prescribed for hypertension control for the last two decades. HQQR can reduce blood pressure in patients with OBH and improve lipid metabolism, insulin resistance, and left ventricular remodelling (Wang et al. 2019; Zhou et al. 2020). The specific molecular mechanisms of HQQR inhibiting myocardial fibrosis are unknown.

The NOD-like receptor with pyrin domain containing-3 (NLRP3) inflammasome is an intracellular protein complex that is indispensable for activating innate immunity and aseptic inflammation (Li et al. 2017; Swanson et al. 2019). NLRP3 can

CONTACT Deyu Fu  fdy650@126.com  Department of Cardiology, Yueyang Hospital of Integrated Traditional Chinese and Western Medicine, Shanghai University of Traditional Chinese Medicine, Shanghai, China

*These authors contributed equally to this work.

© 2021 The Author(s). Published by Informa UK Limited, trading as Taylor & Francis Group.

This is an Open Access article distributed under the terms of the Creative Commons Attribution-NonCommercial License (<http://creativecommons.org/licenses/by-nc/4.0/>), which permits unrestricted non-commercial use, distribution, and reproduction in any medium, provided the original work is properly cited.

be stimulated by danger-associated molecular patterns (DAMPs), such as silica, uric acid crystals, and pathogen-associated molecular patterns (PAMPs) (Yang et al. 2019). The NLRP3 inflammasome is involved in obesity-related myocardial remodelling and dysfunction by mediating adipose tissue inflammation and promoting metabolic inflammation (Toldo and Abbate 2018). The maturation and secretion of interleukin (IL)-1 β cause the proliferation and activation of cardiac fibroblasts (CFs) and lead to myocardial fibrosis (Li et al. 2017). In mouse models of angiotensin II (Ang II)-induced hypertension, cardiac fibrosis, cardiac remodelling, high NLRP3 expression, and cardiac inflammation are observed (Gan et al. 2018). The NLRP3 inflammasome might be a promising target for the management of myocardial remodelling.

Hence, this study examines whether the effects of HQQR on OBH-related myocardial fibrosis are regulated through the NLRP3 inflammasome pathway. The results could provide some clues for the development of therapeutic strategies against myocardial fibrosis.

Materials and methods

Animals and HQQR recipe

Five-week-old Wistar strain spontaneously hypertensive rats (SHR, $n = 78$, male) and age-matched Wistar-Kyoto strain rats (WKY, $n = 6$, male) were bought from the Beijing Vital River Laboratory Animal Technology Co., Ltd. [license number: SCXK (Beijing) 2016-0006]. They were maintained at the experimental animal centre of Yueyang Hospital of Integrated Traditional Chinese and Western Medicine at a controlled temperature ($22 \pm 2^\circ\text{C}$) and relative humidity (50–60%). This animal study was approved by the Animal Care and Use Committee of Yueyang Hospital of Integrated Traditional Chinese and Western Medicine and conformed to the standards outlined in the National Institutes of Health's Guide for Laboratory Animals Care and Use. Valsartan capsules (Beijing Novartis Pharmaceutical Co., Ltd., batch number X2375) were provided by Novartis (Bale, Switzerland).

HQQR preparation

HQQR was prepared by the Department of Pharmacy of the Eastern Theatre General Hospital of the People's Liberation Army (Nanjing, China). HQQR consisted of *Salvia miltiorrhiza* Bunge (Lamiaceae) 2.4 kg, *Ligusticum chuanxiong* Hort (Umbelliferae) 1.44 kg, *Uncaria angustifolia* (Bertol.) Kuntze (Rubiaceae) 2.4 kg, Stone Cassia 4.8 kg, Mulberry parasite 2.4 kg, *Hawthorn* (Rosaceae) 2.4 kg, and corn whisker 4.8 kg. The details of the plants and their parts used to prepare HQQR are listed in Table 1. The detailed HQQR powder was prepared as follows. Stone Cassia was added to water to decoct for 1 h. The other ingredients, except *U. angustifolia*, were added to decoct two

times. The first was decocted with 10 volumes of water for 1 h. The second time was decocted with eight volumes of water for 40 min. The decoctions were combined, precipitated, and filtered, and the supernatant was retained. The decoctions were added to *U. angustifolia* and eight volumes of water, decocted for 40 min, filtered, left overnight, and then filtered again. They were concentrated to a proper amount, placed in a vacuum drying oven, vacuum-dried at 80°C , and crushed through a 100-mesh sieve to obtain 3.45 kg of fine powder.

OBH modelling and treatments

After 1 week of acclimation, 72 SHRs were randomly selected to receive a high-fat diet (HFD) made of 45.0% fat, 37.3% carbohydrate, and 17.7% protein. The other six SHRs and six WKY rats were fed a normal diet (ND) made of 13.6% fat, 63.4% carbohydrate, and 23.0% protein. The ND (#P1101F) and HFD (#MDDZ003) were purchased from Jiangsu Medicine Bio-Pharmaceutical Co., Ltd. After 10 weeks of feeding with HFD, the 24 SHRs with the highest body weight were determined as OBH rats (Levin 1999). Together with the WKY group fed with ND ($n = 6$) and the SHR group fed with ND ($n = 6$), the OBH rats were divided into four groups for studying the effect of HQQR *in vivo*: OBH group fed with HFD ($n = 6$), OBH + HQQR(L) group fed with HFD and given 19.35 g/kg/d of HQQR crude drug intragastrically ($n = 6$), OBH + HQQR(H) group fed with HFD and given 38.7 g/kg/d of HQQR crude drug intragastrically ($n = 6$), and OBH + valsartan group fed with HFD and given 30 mg/kg/d of valsartan intragastrically ($n = 6$). The whole process lasted 10 weeks.

Physiological and morphological indexes

The tail-cuff method was used to monitor systolic blood pressure (SBP) and heart rate (HR) (BP-98A, Beijing Softron Biotechnology Co., Ltd, China) every 2 weeks after treatment. The rats were warmed at 35°C for 5 min before measurement, and each measurement was repeated three times (Erken et al. 2013). The body weight was measured every 2 weeks. The nasal canal length (cm) was measured after treatment. Lee's index was calculated to evaluate the degree of obesity: Lee's index = $\sqrt[3]{\text{body weight (g)} \times 10^3 / \text{body length (cm)}}$ (Hariri and Thibault 2010).

Assessment of cardiac remodelling

After 10 weeks of treatment, echocardiography was performed to assess cardiac function. After rats were anaesthetized with 2% isoflurane, the chest was shaved, and the following parameters were measured with a Vevo 2100 high-resolution *in vivo* microimaging system (Visual Sonics Inc., Toronto, Canada): interventricular septal thickness (IVSD), left ventricular internal diameter at end-diastole (LVIDd), and left ventricular posterior wall

Table 1. Plants used for the Huoxue Qianyang Qutan recipe.

Binominal name	Family	Genus	Species	Parts used	Amount used (kg)
<i>Salvia miltiorrhiza</i>	Lamiaceae	<i>Salvia</i> Linn	<i>S. miltiorrhiza</i>	Root	2.4
<i>Ligusticum chuanxiong</i>	Apiaceae	<i>Ligusticum</i> L.	<i>Apiales</i>	Dry rhizome	1.44
<i>Uncaria angustifolia</i>	Asteraceae	<i>Echinacea</i>	<i>E. angustifolia</i>	Dry with hook stem branches	2.4
<i>Stone cassia</i>	Haliotidae	<i>Haliotis</i>	<i>Concha haliotidis</i>	The shell of abalone	4.8
Mulberry parasite	Loranthaceae	<i>Taxillus</i> Van Tiegh	<i>Parasitic loranthus</i>	Dry leafy stems and branches	2.4
Hawthorn	Rosaceae	<i>Crataegus</i>	<i>Crataegus rhipidophylla</i>	Dry ripe fruit	2.4
Corn whisker	Poaceae	<i>Zea</i>	<i>Zea mays</i> L.	Styles and stigmas of maize	4.8

thickness in diastole (LVPWd). The corrected left ventricular mass (LVM-cor) was automatically calculated. Subsequently, the rats were euthanized for collecting abdominal aorta blood, and the heart and liver tissues were quickly obtained. The left ventricle tissues were separated and weighed. The left ventricular mass index (LVMI), heart weight/body weight (HW/BW), and heart weight/tibia length (HW/TL) were evaluated.

Histological analysis

Cardiac specimens were fixed in 4% paraformaldehyde for 24 h, embedded in paraffin the next day, and sectioned. Haematoxylin and eosin (HE) staining and Masson trichrome staining were performed according to a standard protocol (Al-Mazroua et al. 2013). For immunohistochemistry (IHC), the sections were rinsed, dewaxed, and prepared as previously described (Li et al. 2017). The primary antibodies were collagen type I (Col I) (AF7001, Affinity, Cincinnati, OH, USA, 1:1000) and collagen type III (Col III) (22734-1-AP, Proteintech, Wuhan, China, 1:2000). The stained samples were observed using an optical microscope (Leica, Germany) and photographed at 400 \times magnification for morphological observation and analysis. Image J 1.48 (National Institutes of Health, Bethesda, MD, USA) was used to calculate the percentage of positive area.

Cell culture and treatment

Primary CFs isolated from 1 to 3-day-old SD rats were cultured as described previously (Dhume et al. 2006). Then, the CFs were maintained in Dulbecco's Modified Eagle Medium (DMEM) containing 10% foetal bovine serum (FBS) in a 37°C incubator with 5% CO₂. Ang II (05-23-0101, Sigma, St Louis, MI, USA) was used to induced cardiac fibrosis. The control group of cells was cultivated with FBS. Another five groups of cells were treated with Ang II (1 μ mol/L), Ang II (1 μ mol/L) + HQQR (1.25 mg/mL), Ang II (1 μ mol/L) + HQQR (1 mg/mL), Ang II (1 μ mol/L) + valsartan (20 μ mol/L) (Al-Mazroua et al. 2013), or Ang II (1 μ mol/L) + caspase-1 inhibitor (Ac-YVAD-CHO) (abs811914, Absin, Shanghai, China) (0.4 μ mol/mL) for 48 h.

Overexpression and knockdown of NLRP3

The cells were transfected with plasmids using Lipofectamine 2000 (Invitrogen Inc., Carlsbad, CA, USA) to overexpress or knockdown NLRP3 in CFs. The pc-DNA3.1 plasmid overexpressing NLRP3 (oeNLRP3) was produced by Genewiz Biotechnology (Suzhou, China). The NLRP3 siRNA and its negative control (siNC) were ordered from Major Bio-Pharmaceutical Technology (Shanghai, China). The sequences of the siNLRP3 were 5'-GGA UCU UUG CAG CGA UCA ATT-3' (sense) and 5'-UUG AUC GCU GCA AAG AUC CTT-3' (antisense). The sequences of siNC were 5'-CAG UAC UUU UGU GUA CAA-3' (sense) and 5'-UUG UAC ACA AAA GUA CUG-3' (antisense). Finally, the cells were treated with Ang II, Ang II + siNLRP3,

Ang II + vector + HQQR, or Ang II + oeNLRP3 + HQQR. The expression of NLRP3 was confirmed by PCR and western blot.

Cell proliferation assay

Cell counting kit-8 (CCK-8) was used to evaluate cell proliferation. A 96-well plate was seeded with 5 \times 10³ cells/well. After being treated under different concentrations of HQQR (0, 0.05, 0.25, 0.50, 0.75, 1, 1.25, 1.50, and 1.75 mg/mL) for 48 h, the cells were mixed with the CCK-8 reagents (CP002, Signalway Antibody LLC, College Park, MD, USA), and incubated in a 5% CO₂ incubator for 1 h at 37°C. The optical density (OD) value was read at 450 nm using a microplate reader (DNM-9602, Prolong, Beijing, China). Subsequently, HQQR 1.25 and 1 mg/mL were selected for the experiments.

Enzyme-linked immunosorbent assay (ELISA)

According to the manufacturer's instructions, IL-1 β (xy-E12689; Xinyu Biological, Shanghai, China) concentrations and hydroxyproline (Hyp) (RA20296; Xinyu Biological, Shanghai, China) content in serum and CFs supernatant were measured with standard ELISA kits. Optical density was read at 450 nm using a microplate reader (DNM-9602, Prolong, Beijing, China).

Cell immunofluorescence

CFs were fixed in 4% paraformaldehyde and permeabilized with 0.5% Triton X-100 in PBS. The CFs were blocked with 1% bovine serum albumin (BSA) in PBS for 1 h. Subsequently, the cells were incubated with primary antibody α -SMA (Abcam, Cambridge, United Kingdom, 1:200) overnight at 4°C. After washing, the cells were incubated with secondary fluorescent antibodies Alexa Fluor 555-labeled Donkey anti-Rabbit IgG (H + L) (Beyotime, Shanghai, China, 1:100) at room temperature for 1 h, and with DAPI (1:500, Abcam, Cambridge, UK) for 10 min at room temperature. All samples were observed with a confocal laser scanning microscope (Nikon, Tokyo, Japan). Image J was used to calculate the positive area.

Real-time quantitative PCR

The total RNA was extracted from heart tissue and CFs using Trizol (1596-026, Invitrogen Inc., Carlsbad, CA, USA). After DNase treatment, the RNA was reverse-transcribed into cDNA using the TaqMan RNA Reverse Transcription Kit (#K1622, Fermentas, Burlington, Canada). The mRNA levels were quantified by SYBR Green Master Mix (#K0223, Thermo Fisher Scientific, Waltham, MA, USA), and the relative mRNA levels were calculated with the 2^{- $\Delta\Delta$ Ct} method. GAPDH was used as an internal control for normalization. The primers are listed in Table 2.

Table 2. Primer sequences.

Target gene	F	R
NLRP3	5' TGTGTGCAGGATCTCGCATTGG 3'	5' TGAGCAGCACAGTGAAGTAAGG 3'
Caspase-1	5' AGTGTAGGGACAATAAATGG 3'	5' GATGGACCTGACTGAAGC 3'
IL-1 β	5' TGTGATGTTCCATTAGAC 3'	5' TCTTTGGGTATTGTTTGG 3'
GAPDH	5' GGAGTCTACTGGCGTCTTAC 3'	5' ATGAGCCCTCCACGATGC 3'

Western blot analysis

Cardiac tissues and CFs were lysed in RIPA lysis buffer (BYL40825, JRDUN Biotechnology, Shanghai, China). The protein concentrations were determined using a BCA protein assay kit (PICPI23223, Thermo Fisher Scientific, Waltham, MA, USA). The total proteins were separated by SDS-PAGE and transferred to polyvinylidene fluoride membranes. The membranes were blocked with 5% non-fat milk for 1 h at room temperature and incubated with the primary antibodies against NLRP3 (19771-1-AP, Proteintech Group Inc., Chicago, IL, USA, 1:1000), caspase-1 (22915-1-AP, Proteintech Group Inc., Chicago, IL, USA, 1:1000), IL-1 β (MAB5011-100, R&D Systems, Minneapolis, MN, USA, 1:500), Col I (AF7001, Affinity BIO, Scoresby, Australia, 1:1000), Col III (22734-1-AP, Proteintech Group Inc., Chicago, IL, USA, 1:1000), and GAPDH (5174S, Cell Signalling Technology, Inc., Danvers, MA, USA, 1:2000) overnight at 4°C. After washing with TBST, the membrane was incubated with horseradish peroxidase-conjugated goat anti-rabbit IgG/HRP secondary antibodies (A0208, Beyotime, Shanghai, China, 1:1000) for 1 h at room temperature. The bands were visualized with enhanced chemiluminescent kit western-blotting detection reagents (Amersham, GE Healthcare, Waukesha, WI, USA) and assessed on a Tanon-5200 system.

Statistical analysis

All data are shown as means \pm standard deviations (SD), and statistical analyses were conducted with SPSS V26.0 (IBM, Armonk, NY, USA). The statistical tests one-way ANOVA analysis and the least significant difference (LSD) test were performed to observe the significant differences between the sample means. $p < 0.05$ was considered statistically significant.

Results

HQQR reduced SBP, HR, body weight, and Lee's index in OBH rats

After HFD exposure for 10 weeks, the colour of the OBH rat's liver became lighter, red, and heavier, indicating more serious fat deposition compared with SHR (Figures 1(A) and 2). In terms of blood pressure, the average SBP values in the OBH + HQQR(H) and OBH + valsartan groups were significantly lower than in the OBH control group (201.67 ± 21.00 vs. 169.00 ± 10.00 ; $p < 0.05$) (Figure 1(B)). After 3 weeks, HQQR showed an anti-hypertension effect, which lasted until the end of treatment, indicating that HQQR had a significant blood pressure reduction effect. However, the antihypertensive effect of HQQR was slightly inferior to valsartan. Compared with OBH, HQQR(H) could also reduce the HR (Figure 1(C)). After 10 weeks, HQQR(H) could reduce the body weight (387.83 ± 10.17 vs. 358.17 ± 6.40 ; $p < 0.05$) and decrease Lee's index (321.50 ± 3.87 vs. 314.58 ± 3.88 ; $p < 0.05$) compared to OBH control group (Figure 1(A,D)).

HQQR alleviated left ventricular hypertrophy (LVH) in OBH rats

As shown in Figure 3(A), OBH rats had increased HW/BW, HW/TL, and LVMI than WKY rats. HQQR(H) alleviated HW/BW (3.69 ± 0.22 vs. 3.25 ± 0.11 ; $p < 0.05$), HW/TL (31.5 ± 1.77 vs. 29.44 ± 1.07 ; $p < 0.05$), and LVMI (3.26 ± 0.27 vs. 2.71 ± 0.12 ;

$p < 0.05$) compared with the OBH group. HQQR(H) had greater effects on HW/BW than HQQR(L) (3.49 ± 0.12 vs. 3.25 ± 0.11 ; $p < 0.05$). HQQR(L) decreased LVMI compared with the OBH group (3.26 ± 0.27 vs. 2.91 ± 0.08 ; $p < 0.05$). Cardiac echocardiography showed that LVM-cor was significantly attenuated in the OBH + HQQR(H) group compared with the OBH group (1129.66 ± 50.28 vs. 952.93 ± 28.7 ; $p < 0.05$) (Figure 3(B,C)). There were no effects on IVSD, LVIDD, and LVPWd.

HQQR attenuated myocardial fibrosis

HE showed that the cardiomyocytes of SHR rats had mild edoema and degeneration, and the myocardial fibres were arranged disorderly. The degree of edoema and degeneration of myocardial cells in rats fed with HFD was more serious with a disorder of myocardial fibres arrangement and inflammatory cell infiltration. HQQR treatment could alleviate myocardial cell edoema, reducing the percentage of fibrosis area (18.99 ± 3.90 vs. 13.37 ± 3.39 ; $p < 0.05$), and reduce inflammatory cell infiltration, reducing IL-1 β in plasma (10.07 ± 1.16 vs. 5.35 ± 1.29 ; $p < 0.05$), and correct myocardial fibres' order. In addition, Masson staining revealed cardiac fibrosis in OBH model rats, accompanied by higher expression of Col I and Col III evaluated by IHC. This was improved after high-dose HQQR and valsartan treatment (Figure 4).

HQQR alleviated Ang II-induced CFs fibrosis in vitro

The effect of HQQR on the proliferation of CFs was evaluated *in vitro* by treating the CFs with different concentrations of HQQR (0, 0.05, 0.25, 0.50, 0.75, 1, 1.25, 1.50, and 1.75 mg/mL) (Figure 5(A)). Then, 1.25 and 1 mg/mL of HQQR were selected for the subsequent experiments based on the IC₅₀ of HQQR (1.396 mg/mL). Considering the critical role of caspase-1 and NLRP3 in cardiac fibrosis (Gao et al. 2019), we evaluated whether they were involved in the mechanism of HQQR in preventing myocardial fibrosis progression. We first applied HQQR and the caspase-1 inhibitor Ac-YVAD-CHO to detect their effect on the proliferation of CFs. Both showed that the Ang II-induced proliferation of CFs and Hyp secretion was significantly reduced by HQQR and Ac-YVAD-CHO (Figure 5(B,C)); proliferation OD value (1.09 ± 0.02 vs. 0.84 ± 0.01 ; $p < 0.05$). The immunofluorescence assay was then performed to detect the expression of the fibrotic marker α -SMA. Higher concentration HQQR (1.25 mg/mL) and Ac-YVAD-CHO significantly reduced the area density of α -SMA (14.74 ± 3.39 vs. 3.97 ± 0.53 ; $p < 0.05$) (Figure 5(D,E)). This suggests that the anti-fibrotic effect of HQQR might be related to caspase-1.

Furthermore, the role of NLRP3 in the mechanism of HQQR was explored. First, we established cell lines with a high or low expression of NLRP3, which were confirmed by polymerase chain reaction (PCR) and western blotting (Figure 6(A)). The CCK8 assay showed that oeNLRP3 could significantly reverse the antiproliferation and Hyp secretion reduction effects of HQQR, whereas siNLRP3 enhanced that activity (Figure 6(B,C)). Correspondingly, the immunofluorescence results showed that the area intensity of α -SMA in fibrotic CFs decreased in the siNLRP3 group compared with the Ang II-treated group oeNLRP3 significantly offset HQQR's effect (Figure 6(D,E)).

Taken together, the data showed that HQQR could blunt cardiac fibrosis development and suppress CF proliferation by interfering with the NLRP3/caspase-1 axis.

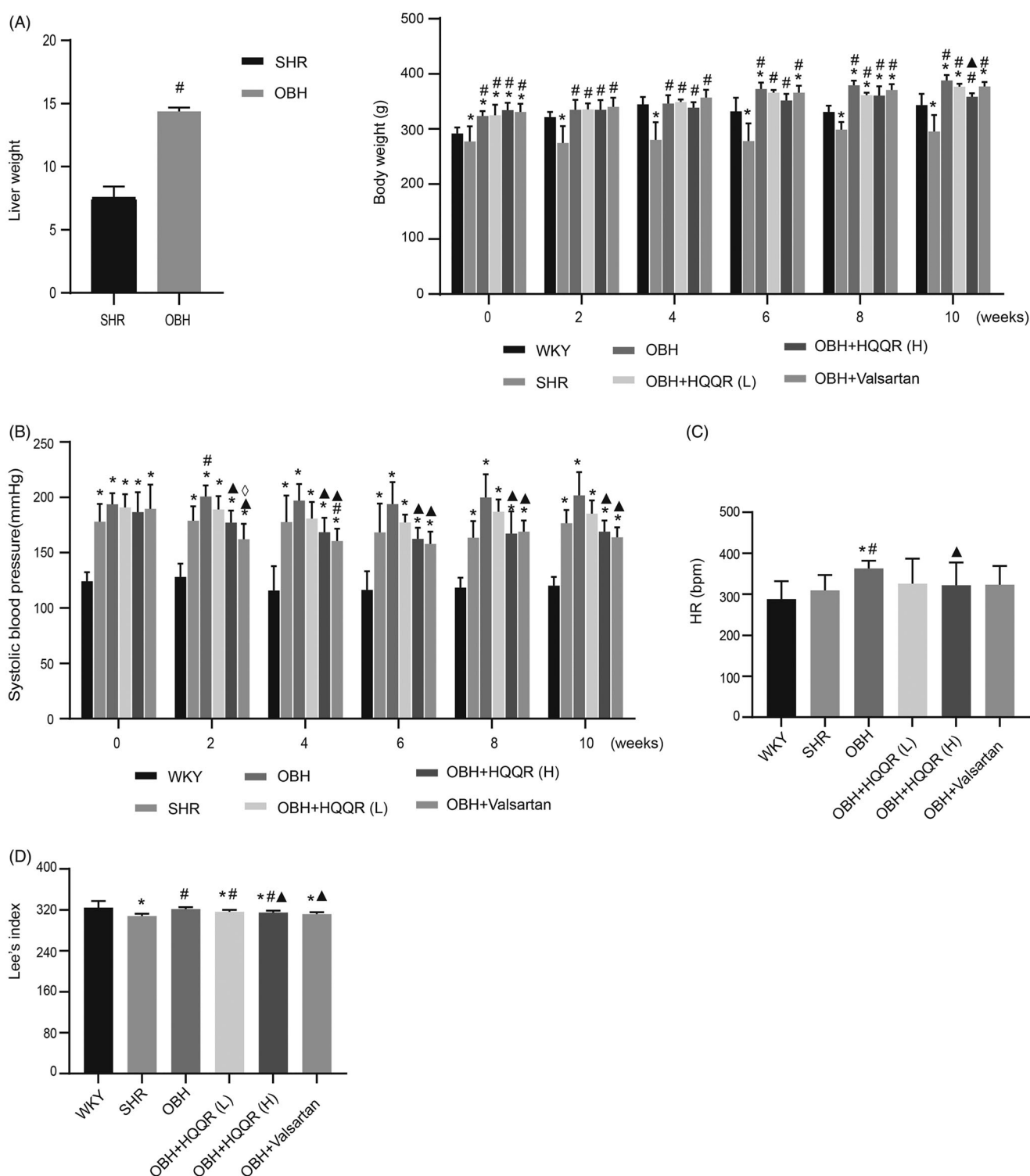


Figure 1. Effects of HQQR on liver and body weight, SBP, HR, and Lee's index. (A) Changes in liver and body weight after HFD exposure for 10 weeks. (B) SBP among the different groups of rats, measured every 2 weeks of treatment, for 10 weeks. (C) Comparison of HR among the different groups after 10 weeks of treatment. (D) Comparison of Lee's index between different groups after 10 weeks of treatment. * $p < 0.05$ vs. WKY group; # $p < 0.05$ vs. SHR group; ▲ $p < 0.05$ vs. OBH group; ◇ $p < 0.05$ vs. OBH + HQQR(L) group.

HQQR downregulated the NLRP3 inflammasome signalling pathway to inhibit cardiac fibrosis in vivo and in vitro

We examined the action of HQQR on the NLRP3 inflammasome signalling pathway in cardiac fibrosis progression. As shown in Figure 7(A), the fibrosis markers Col I and Col III (protein expression) were increased by Ang II; Col I (0.50 ± 0.02 vs. 0.27 ± 0.05 ; $p < 0.05$), and Col III (0.48 ± 0.21 vs. 0.26 ± 0.11 ,

$p < 0.05$). However, it could be mitigated by a high or low concentration of HQQR. The caspase-1 inhibitor or siNLRP3 also attenuated the expression of Col I and Col III. Then, the expression of IL-1 β was detected both *in vitro* and *in vivo*. Ang II-induced CFs showed a high secretion of IL-1 β in the culture supernatant. In contrast, IL-1 β secretion was decreased by HQQR (both low and high concentrations), the caspase-1

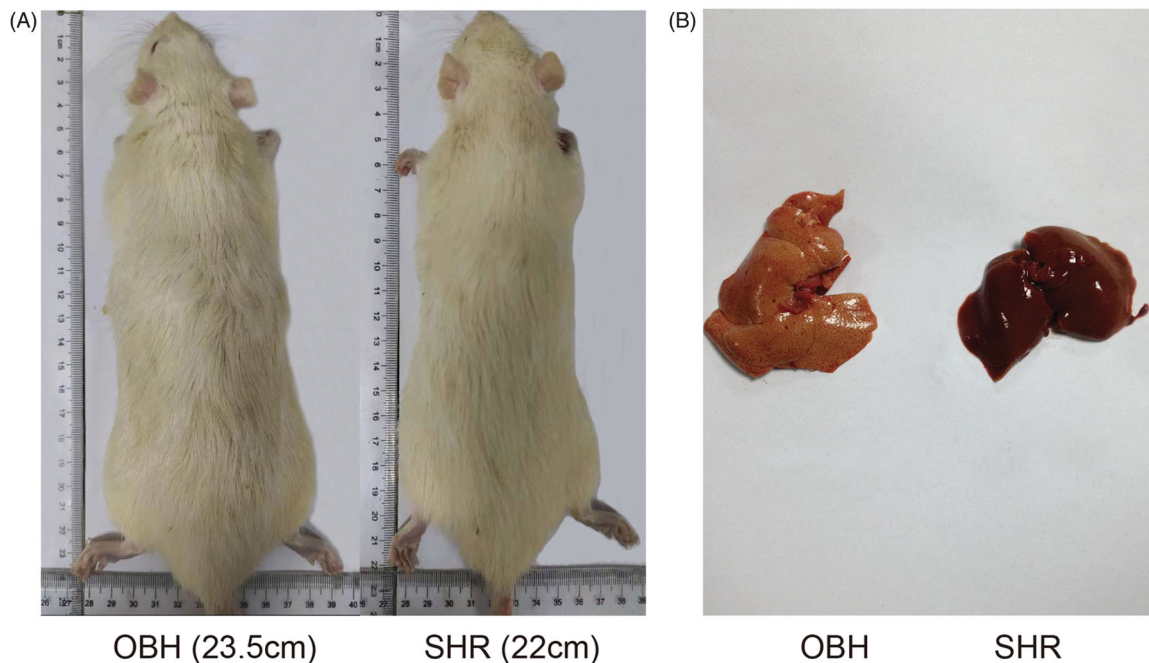


Figure 2. (A) Morphological change of OBH rats compared with SHR rats after HFD exposure for 10 weeks. (B) Different sizes and colours of livers compared with SHR rats after 10 weeks of HFD exposure.

inhibitor, and si-NLRP3 (Figure 7(B)). Ang II treatment stimulated NLRP3 expression in CFs, downregulated by HQQR (both low and high concentrations), the caspase-1 inhibitor, and si-NLRP3. Also, HQQR, siNLRP3, and the caspase-1 inhibitor decreased cleaved caspase-1 concentration and mature IL-1 β mRNA and protein levels (Figure 7(C,D)). Therefore, the activation of NLRP3 plays an important role in the induction of cardiac fibrosis. HQQR alleviated myocardial fibrosis by inhibiting the NLRP3 inflammasome pathway *in vitro*. *In vivo*, we showed that the levels of matured IL-1 β were high in the serum of OBH rats, but IL-1 β expression was significantly downregulated after treatment with HQQR or valsartan (Figure 8(A)). The OBH group had higher levels of NLRP3 mRNA in the myocardium than the WKY and SHR groups, and HQQR and valsartan decreased the NLRP3 mRNA levels (Figure 8(B)). Consistent with the *in vitro* result, the protein expression of NLRP3 and IL-1 β in the myocardium was reduced after HQQR treatment, while caspase-1 showed a downward trend (Figure 8(C)). Taken together, we demonstrated that NLRP3/caspase-1/IL-1 β signalling pathway was involved in the protective effect of HQQR, both *in vivo* and *in vitro*.

Discussion

HQQR is used to manage hypertension and can improve cardiac remodelling, but the mechanisms are poorly understood. This study aimed to examine whether the effects of HQQR on OBH-related myocardial fibrosis are mediated through the NLRP3 inflammasome pathway. The results showed that HQQR could blunt the development of cardiac fibrosis and suppress CF proliferation by directly interfering with the NLRP3/caspase-1/IL-1 β pathway. Hence, HQQR could be a promising approach for the treatment of cardiac damage in OBH.

In this study, the diet-induced obesity hypertension model (45.0% calories from fat) was used to exam the effects of OBH on the myocardium. Consistently with observations in humans (Non-Communicable Disease Risk Factor [NCDRF] 2016; Afshin

et al. 2017), the OBH models showed increased blood pressure, visceral fat deposition, and weight gain. On the other hand, this study showed that HQQR lowered Lee's index of the OBH model, partially alleviating obesity.

Inflammation participates in metabolic-related diseases, including obesity, T2DM, and atherosclerosis. The NLRP3 inflammasome plays a prominent part in the initiation and progression of inflammation and related diseases (Pejnovic et al. 2013; Patel et al. 2015). The activation of NLRP3 can recruit ASC and caspase-1 to form a multi-protein complex called 'inflammasome'. This activation leads to self-cleavage and activation of caspase-1 and subsequently cleaves pro-IL-1 β and pro-IL-18 to their biologically active forms. These are involved in the pathogenesis of many chronic diseases (van Hout et al. 2017). In the present study, the OBH models showed increased NLRP3, caspase-1, and IL-1 β , as expected. *In vivo*, HQQR could reduce the expression of NLRP3, caspase-1, and IL-1 β , indicating the HQQR exerts its effects, at least in part, through decreasing the NLRP3 axis.

Inflammation plays an important role in cardiac remodelling progression in obesity, hypertension, ischemia/reperfusion injury, myocardial infarction, and diabetic cardiomyopathy (Gan et al. 2018; Wang et al. 2019; Zhou et al. 2020). Myocardial fibrosis is a hallmark of myocardial remodelling in obesity and hypertension, reflecting abnormalities of extracellular matrix (ECM) synthesis and degradation (Talman and Ruskoaho 2016). There is increasing evidence that the NLRP3 inflammasome signal can mediate fibrotic diseases by promoting the profibrotic phenotype of various cells via IL-1 β (Peng et al. 2020). Local secretion of IL-1 β can enhance inflammatory response and promote the process of myocardial fibrosis (Ren et al. 2020) by regulating ECM metabolism and thus fibroblast function (Jia et al. 2016). Our results showed progressive cardiac fibrosis and activation of NLRP3/caspase-1 cascade in the OBH model, which led to the secretion of mature IL-1 β pro-inflammatory factor. High-dose HQQR could alleviate cardiac fibrosis, improve ECM deposition, inhibit NLRP3 inflammasome activation, and matured IL-1 β

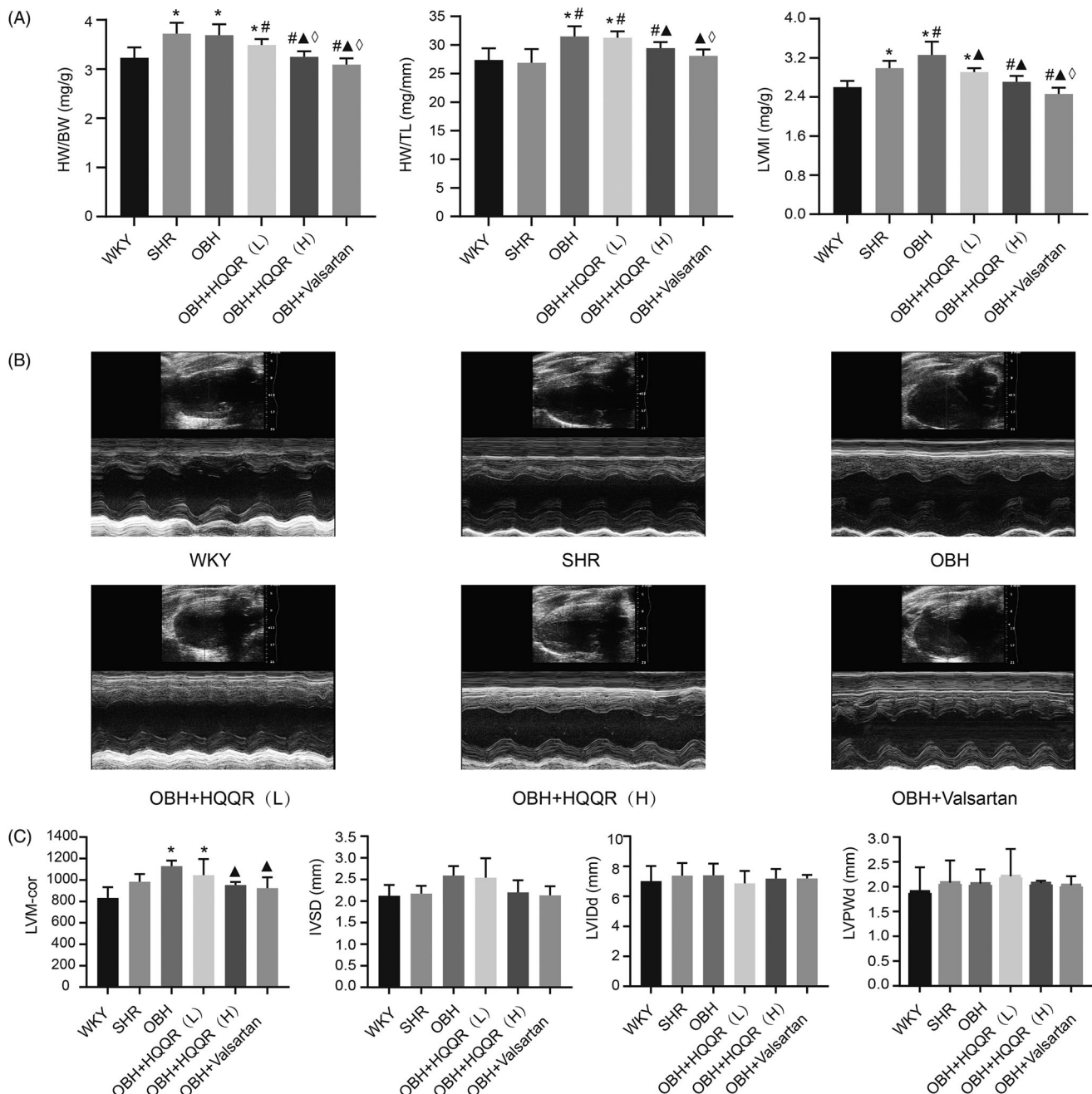


Figure 3. HQQR alleviated LVH in OBH rats. (A) Measurements of heart weight/body weight (HW/BW), heart weight/tibia length (HW/TL), and left ventricle mass/body weight (LVMI) after 10 weeks of treatment. (B) Representative images of cardiac echocardiography after 10 weeks of treatment. (C) Left ventricular mass (LVM-cor), interventricular septal thickness (IVSD), left ventricular internal diameter at end-diastole (LVIDd) and left ventricular posterior wall thickness in diastole (LVPWd). * $p < 0.05$ vs. WKY group; # $p < 0.05$ vs. SHR group; $\blacktriangle p < 0.05$ vs. OBH group; $\diamond p < 0.05$ vs. OBH + HQQR(L) group.

release *in vitro* experiment, which is a potential treatment for myocardial fibrosis.

CFs are the key cells responsible for the occurrence and development of cardiac fibrosis (Krenning et al. 2010). CFs proliferate dramatically in pathological states, causing ECM metabolic balance by secreting collagen. During fibrosis development, the collagen fibres, especially Col I and Col III proteins, excessively accumulate in myocardial tissues (González et al. 2020), damaging the cardiac systolic and diastolic functions (Jia et al. 2016). Non-immune cells, such as CFs can assemble and spark off the NLRP3 inflammasome for the duration of the development of cardiomyopathies (Sandanger et al. 2013).

The expression of myocardial NLRP3 increased 3-fold after injection of Ang II into mice, accompanied by macrophage aggregation and myocardial fibrosis (Willeford et al. 2018). Increasing evidence indicates that blocking NLRP3 activation can reduce IL-1 β production in macrophages, inhibit the transformation of myocardial fibroblasts into myofibroblasts, and reduce myocardial inflammation and fibrosis in Ang II-induced hypertensive rats (Gan et al. 2018). It was observed in the present study *in vivo* that Ang II-induced NLRP3 inflammasome activation and subsequent IL-1 β release in CFs. This could be attenuated by valsartan (an Ang II receptor antagonist), supporting the notion that Ang II is an important stimulus of NLRP3. Besides,

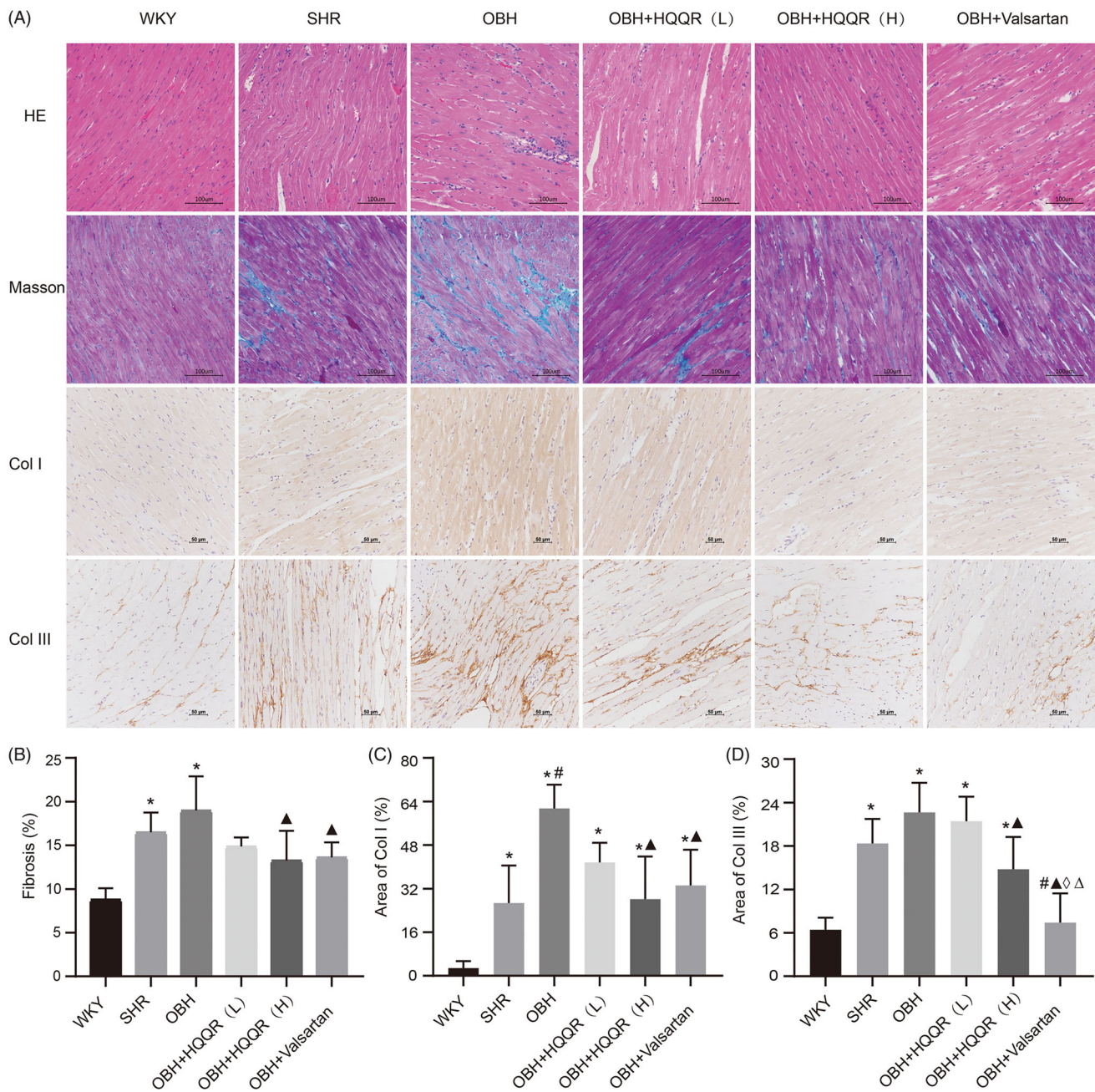


Figure 4. HQQR treatment alleviated myocardial fibrosis. (A) Representative photomicrographs of HE, Masson's staining, and IHC (Col I and Col III) of the myocardium of rats. (B) The area of fibrosis in the myocardium was calculated using the Image J software. (C) The area of Col I in the myocardium was calculated using the Image J software. (D) The area of Col III in the myocardium was calculated using the Image J software. * $p < 0.05$ vs. WKY group; # $p < 0.05$ vs. SHR group; ▲ $p < 0.05$ vs. OBH group; ◇ $p < 0.05$ vs. OBH + HQQR(L) group; △ $p < 0.05$ vs. OBH + HQQR(H) group.

either knockout of NLRP3 or caspase-1 inhibitor treatment reduced the mature IL-1 β release, accompanied by decreased ECM deposition and α -SMA expression. HQQR displayed a similar inhibitory effect on fibrosis, which was reversed by the overexpression of NLRP3 *in vivo*. In contradiction with the present study, a study reported that NLRP3 deficiency accelerated pressure overload-induced cardiac remodeling in mice (Disma et al. 2018). This discrepancy is likely due to the use of different mice and rat models. Moreover, this study did not examine the function of CFs *in vitro*. Based on these findings, the NLRP3 inflammasome might play bidirectional roles in cardiac damage of different models.

Previous studies by the authors' group showed that HQQR could alleviate endoplasmic reticulum stress (ERS) (Zhou et al.

2020) and down-regulate mitochondrial reactive oxygen species (ROS) in cardiac damage of OBH models (Pejnovic et al. 2013). The NLRP3 inflammasome activation is induced by various signals that lead to priming and activation, a two-stage process (Yin et al. 2009). The nuclear factor κ B (NF- κ B) can induce NLRP3 and pro-IL-1 β expression (Bekhat et al. 2017). The activation of the NLRP3 inflammasome related to ERS is followed by the activation of NF- κ B (Kim et al. 2014). ERS acts as the endogenous stimulator of NLRP3 inflammasome through multiple pathways, including the unfolded protein response (UPR), calcium or lipid metabolism, and ROS generation. The NLRP3 inflammasome activation also promotes ROS production and mitochondrial dysfunction (Zhao et al. 2015), which can trigger the occurrence of endoplasmic reticulum stress (ERS) (Wang et al. 2015). The

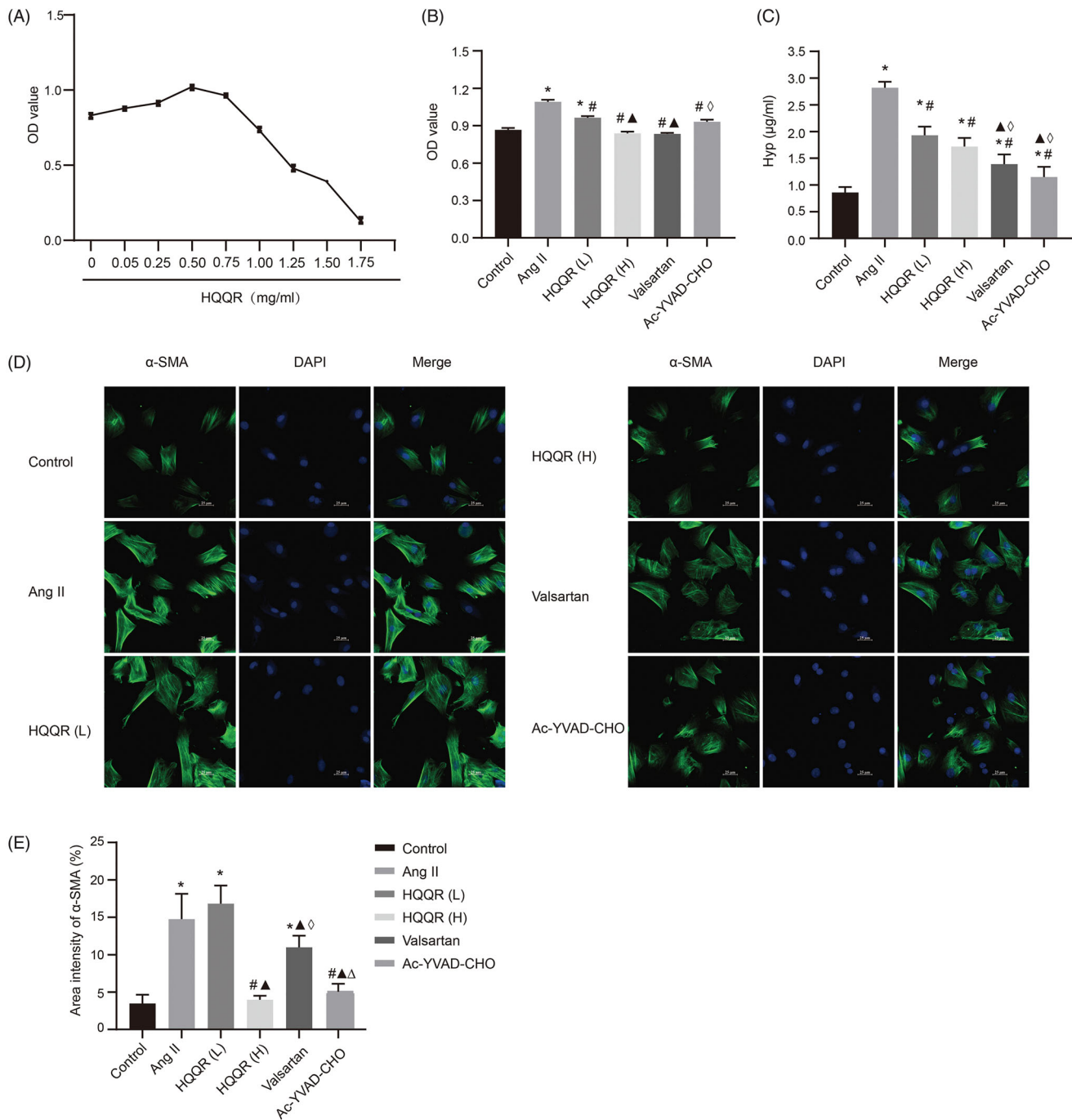


Figure 5. HQQR inhibited the proliferation of CFs and reduced Hyp levels. (A) The proliferation of CFs with different concentrations of HQQR. (B) Effects of HQQR and caspase-1 inhibitor on the proliferation of CFs, measured using the CCK-8 assay. (C) The effects of HQQR and caspase-1 inhibitor on Hyp levels. (D) HQQR and caspase-1 inhibitor effects on the density of α -SMA measured immunofluorescence staining under a laser scanning confocal microscope. (E) Area intensity of α -SMA was quantified by image J. * $p < 0.05$ vs. control group; # $p < 0.05$ vs. Ang II group; ▲ $p < 0.05$ vs. HQQR(L) group; ◇ $p < 0.05$ vs. HQQR(H) group; △ $p < 0.05$ vs. valsartan group.

release of Ca^{2+} resulting from ERS ultimately results in mitochondrial damage and further aggravates IL-1 β production downstream of the NLRP3 pathway (Ji et al. 2019). The effects of HQQR on these factors should be explored in future studies.

Since the NLRP3 pathway is of great importance for myocardial remodelling, pharmacological inhibitors targeting the NLRP3 inflammasome or its downstream IL-1 β may be a proper treatment to prevent adverse cardiovascular diseases (CVDs) (Xia et al. 2019; Wang et al. 2020). HQQR, as a treatment for hypertension, may exert its therapeutic actions of

LVH in OBH rats by targeting the myofibroblast NLRP3 inflammasome. The clinical application of HQQR will be further explored in the future.

Nevertheless, the potential limitation of this study is that it is still unclear which ingredient or combination of ingredients in HQQR accounts for reversing fibrosis. Because adipose tissue dysfunction and the IL-1 β secretion is an important link to cardiometabolic diseases, future studies should focus on adipose tissue inflammasome to elucidate the mechanism for the effect of HQQR in cardiac remodelling.

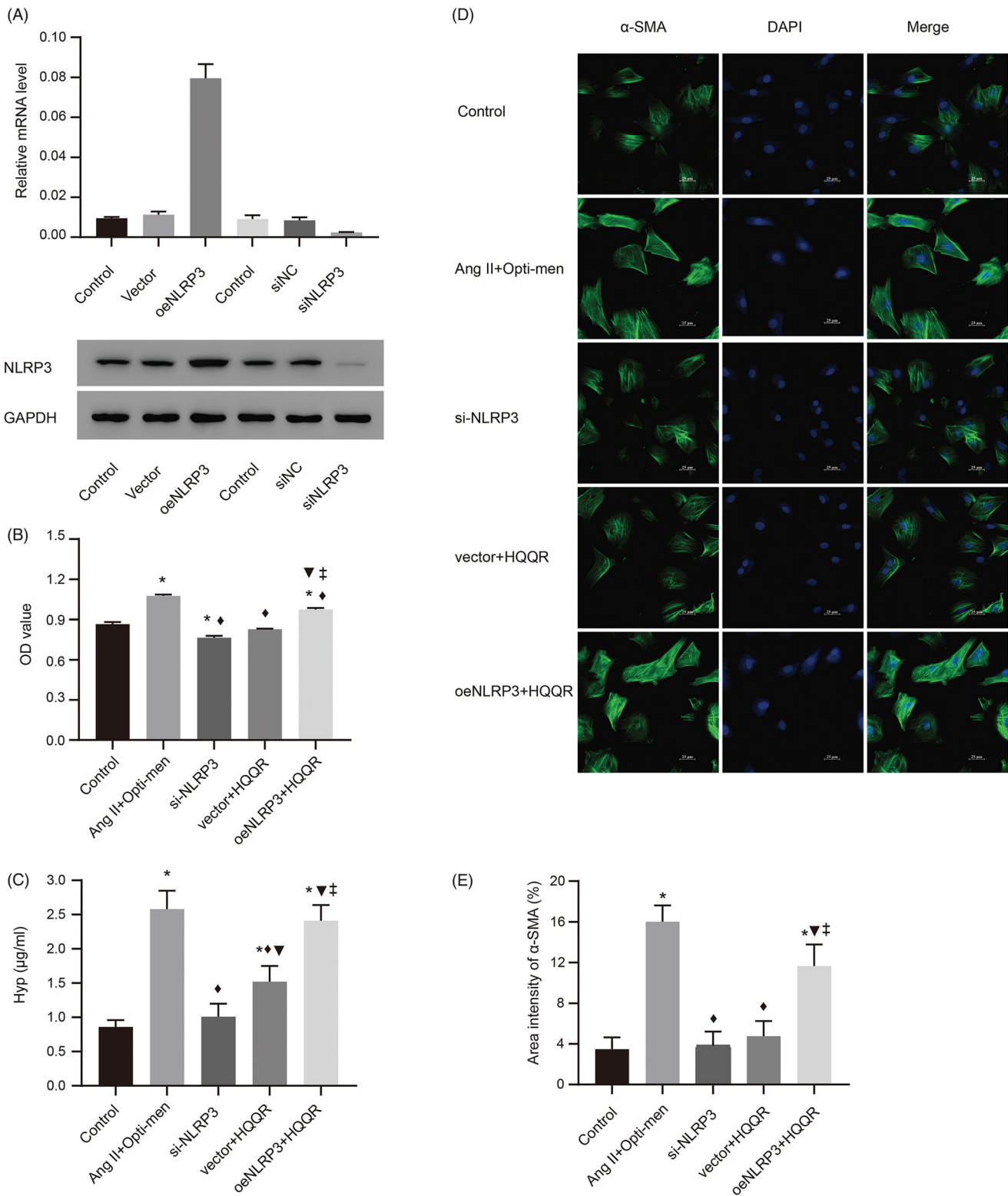


Figure 6. NLRP3 played an important role in the HQQR mediated effect of cardiac fibrosis inhibition. (A) Validation of mRNA and protein expression of NLRP3. (B) Effects of si-NLRP3 and oeNLRP3 on the proliferation of CFs, measured using the CCK8 assay. (C) Effects of si-NLRP3 and oeNLRP3 on Hyp expression. (D,E) The density of α -SMA was observed by immunofluorescence staining under a laser scanning confocal microscope. Area intensity of α -SMA was quantified by image J. * $p < 0.05$ vs. control group; $\blacklozenge p < 0.05$ vs. Ang II + Opti-men group; $\blacktriangledown p < 0.05$ vs. si-NLRP3 group; $\ddagger p < 0.05$ vs. vector + HQQR group.

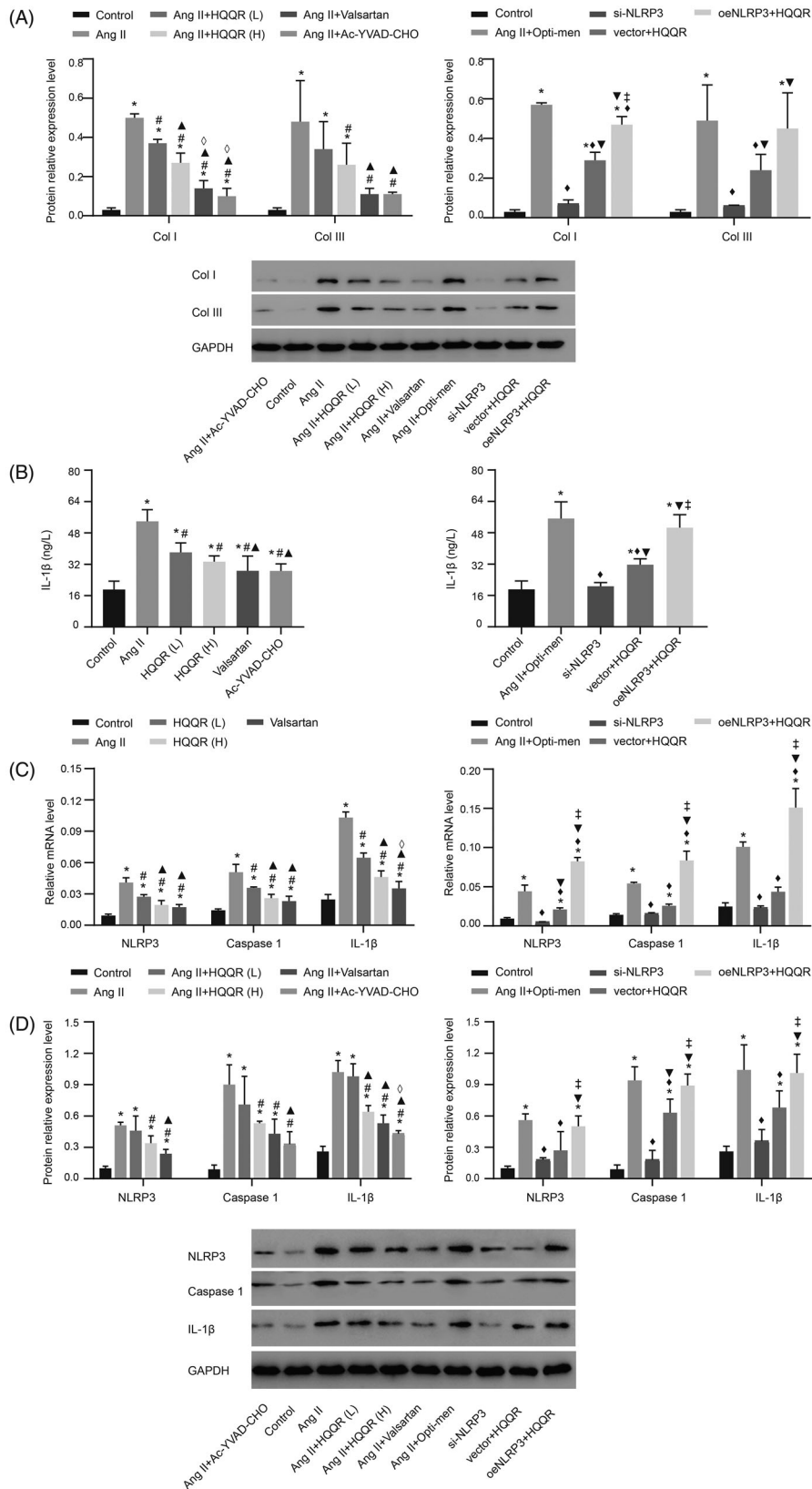


Figure 7. HQQR attenuated CF fibrosis via the NLRP3 inflammasome. (A) The protein expression of Col I and Col III was analyzed by western blotting. (B) The expression of IL-1 β in the supernatant of the different groups of CFs. (C) The mRNA expression of NLRP3, caspase-1, and IL-1 β was analyzed by western blotting. (D) The relative protein expression levels of NLRP3, caspase-1, and IL-1 β among the different groups were quantified using the Image J software. * $p < 0.05$ vs. control group; # $p < 0.05$ vs. Ang II group; $\blacktriangle p < 0.05$ vs. HQQR(L) group; $\square p < 0.05$ vs. HQQR(H) group; $\blacklozenge p < 0.05$ vs. Ang II + Opti-men group; $\blacktriangledown p < 0.05$ vs. si-NLRP3 group; $\ddagger p < 0.05$ vs. vector + HQQR group.

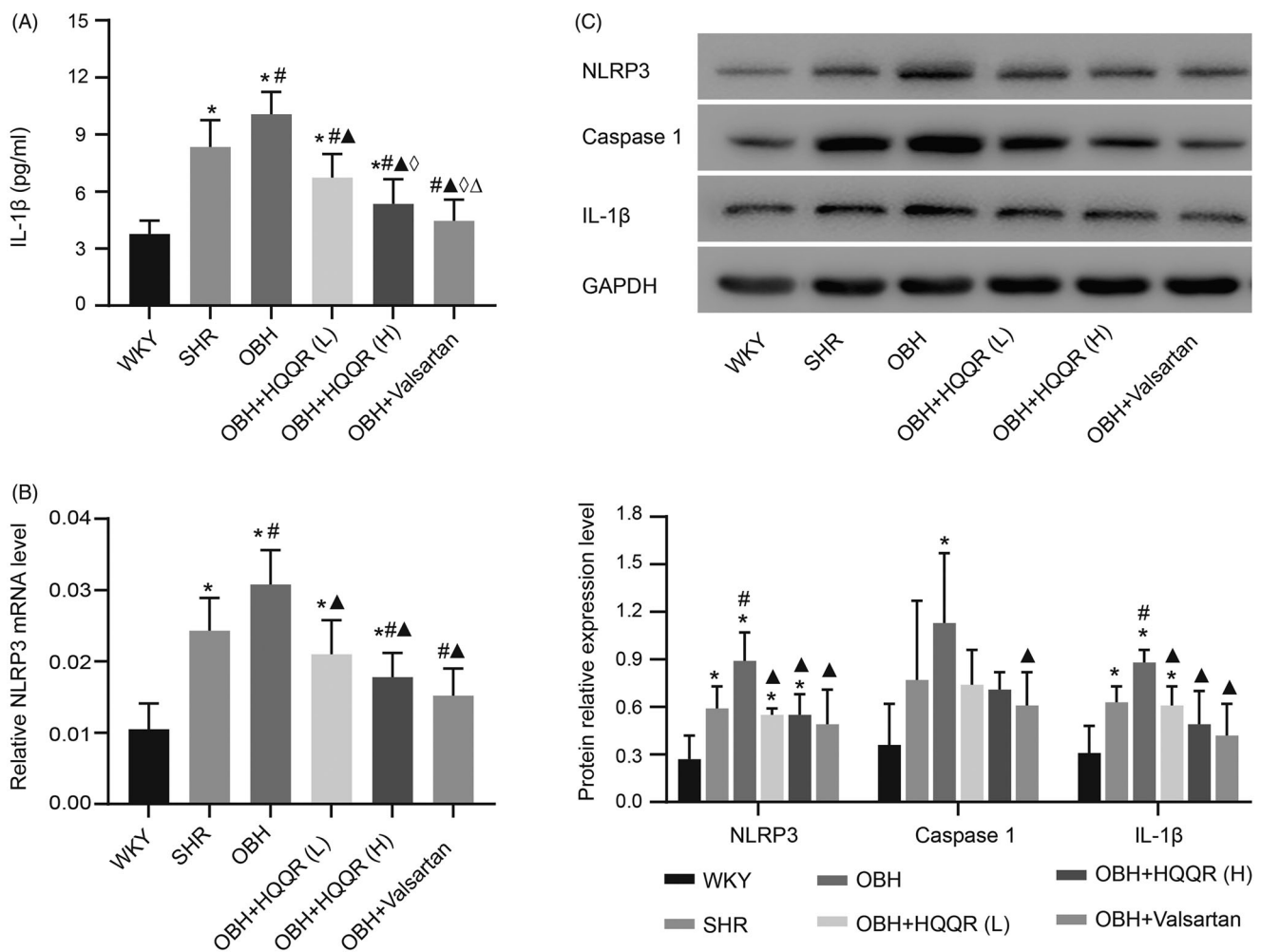


Figure 8. HQQR could reduce the expression of NLRP3 and IL-1 β protein in the rat myocardium. (A) Expression of IL-1 β in the serum in different groups measured by ELISA. (B) The relative NLRP3 mRNA levels were quantified by RT-PCR. (C) NLRP3, caspase-1, and IL-1 β protein expression was analyzed by western blotting and quantified. * $p < 0.05$ vs. WKY group; # $p < 0.05$ vs. SHR group; ▲ $p < 0.05$ vs. OBH group; ◇ $p < 0.05$ vs. OBH + HQQR(L) group; △ $p < 0.05$ vs. OBH + HQQR(H) group.

Conclusions

The present study provides strong evidence that HQQR could blunt cardiac fibrosis development and suppress CF proliferation by directly interfering with the NLRP3/caspase-1/IL-1 β pathway. Hence, HQQR could be a promising approach for the treatment of cardiac damage in OBH.

Disclosure statement

The authors declare that the research was conducted in the absence of any commercial or financial relationships that could be construed as a potential conflict of interest.

Funding

This study was funded by the National Nature Science Foundation of China [grant number 81803892], the National Nature Science Foundation of China [grant number 81774111], the Scientific Research Project of Shanghai Science and Technology Commission [grant number 19401970400], and Shanghai University of Traditional Chinese Medicine [Graduate Innovative Training] Special Scientific Research Project [grant number Y2021035].

Data availability statement

All data generated or analyzed during this study are included in this published article.

References

- Afshin A, Forouzanfar MH, Reitsma MB, Sur P, Estep K, Lee A, Marczak L, Mokdad AH, Moradi-Lakeh M, Naghavi M, et al. 2017. Health effects of overweight and obesity in 195 countries over 25 years. *N Engl J Med.* 377(1):13–27.
- Al-Mazroua HA, Al-Rasheed NM, Korashy HM. 2013. Downregulation of the cardioprotectin-1 gene expression by valsartan and spironolactone in hypertrophied heart rats *in vivo* and rat cardiomyocyte H9c2 cell line *in vitro*: a novel mechanism of cardioprotection. *J Cardiovasc Pharmacol.* 61(4):337–344.
- Aurigemma GP, de Simone G, Fitzgibbons TP. 2013. Cardiac remodeling in obesity. *Circ Cardiovasc Imaging.* 6(1):142–152.
- Bekhat M, Rowson SA, Neigh GN. 2017. Checks and balances: the glucocorticoid receptor and NF κ B in good times and bad. *Front Neuroendocrinol.* 46:15–31.
- Bluhm M. 2019. Obesity: global epidemiology and pathogenesis. *Nat Rev Endocrinol.* 15:288–298.
- Chooi Y, Ding C, Magkos F. 2019. The epidemiology of obesity. *Metabolism.* 92:6–10.
- Dhume A, Lu S, Horowitz R. 2006. Targeted disruption of N-RAP gene function by RNA interference: a role for N-RAP in myofibril organization. *Cell Motil Cytoskeleton.* 63(8):493–511.

- Disma N, O'Leary JD, Loepke AW, Brambrink AM, Becke K, Clausen NG, De Graaff JC, Liu F, Hansen TG, McCann ME, et al. 2018. Anesthesia and the developing brain: a way forward for laboratory and clinical research. *Paediatr Anaesth*. 28(9):758–763.
- Erken HA, Erken G, Genç O. 2013. Blood pressure measurement in freely moving rats by the tail cuff method. *Clin Exp Hypertens*. 35(1):11–15.
- Frangogiannis N. 2019. Cardiac fibrosis: Cell biological mechanisms, molecular pathways and therapeutic opportunities. *Mol Aspects Med*. 65:70–99.
- Gan W, Ren J, Li T, Lv S, Li C, Liu Z, Yang M. 2018. The SGK1 inhibitor EMD638683, prevents Angiotensin II-induced cardiac inflammation and fibrosis by blocking NLRP3 inflammasome activation. *Biochim Biophys Acta Mol Basis Dis*. 1864(1):1–10.
- Gao R, Shi H, Chang S, Gao Y, Li X, Lv C, Yang H, Xiang H, Yang J, Xu L, et al. 2019. The selective NLRP3-inflammasome inhibitor MCC950 reduces myocardial fibrosis and improves cardiac remodeling in a mouse model of myocardial infarction. *Int Immunopharmacol*. 74:105575.
- Global Burden of Diseases, Injuries, and Risk Factors Study (GRF). 2020. Global burden of 87 risk factors in 204 countries and territories, 1990–2019: a systematic analysis for the Global Burden of Disease Study 2019. *Lancet*. 396:1223–1249.
- González A, López B, Ravassa S, San José G, Díez J. 2020. Reprint of “The complex dynamics of myocardial interstitial fibrosis in heart failure. Focus on collagen cross-linking”. *Biochim Biophys Acta Mol Cell Res*. 1867(3):118521.
- Hariri N, Thibault L. 2010. High-fat diet-induced obesity in animal models. *Nutr Res Rev*. 23(2):270–299.
- Hinderer S, Schenke-Layland K. 2019. Cardiac fibrosis – a short review of causes and therapeutic strategies. *Adv Drug Deliv Rev*. 146:77–82.
- Ji T, Han Y, Yang W, Xu B, Sun M, Jiang S, Yu Y, Jin Z, Ma Z, Yang Y, et al. 2019. Endoplasmic reticulum stress and NLRP3 inflammasome: crosstalk in cardiovascular and metabolic disorders. *J Cell Physiol*. 234(9):14773–14782.
- Jia G, DeMarco VG, Sowers JR. 2016. Insulin resistance and hyperinsulinaemia in diabetic cardiomyopathy. *Nat Rev Endocrinol*. 12(3):144–153.
- Kim S, Joe Y, Jeong SO, Zheng M, Back SH, Park SW, Ryter SW, Chung HT. 2014. Endoplasmic reticulum stress is sufficient for the induction of IL-1 β production via activation of the NF- κ B and inflammasome pathways. *Innate Immun*. 20(8):799–815.
- Krenning G, Zeisberg EM, Kalluri R. 2010. The origin of fibroblasts and mechanism of cardiac fibrosis. *J Cell Physiol*. 225(3):631–637.
- Levin BE. 1999. Arcuate NPY neurons and energy homeostasis in diet-induced obese and resistant rats. *Am J Physiol*. 276(2):R382–R387.
- Li R, Lu K, Wang Y, Chen M, Zhang F, Shen H, Yao D, Gong K, Zhang Z. 2017. Triptolide attenuates pressure overload-induced myocardial remodeling in mice via the inhibition of NLRP3 inflammasome expression. *Biochem Biophys Res Commun*. 485(1):69–75.
- Marczak L, Williams J, Loeffler M, For the Institute for Health Metrics and Evaluation. 2018. Global deaths attributable to high systolic blood pressure, 1990–2016. *JAMA*. 319(21):2163.
- Non-Communicable Disease Risk Factor (NCDRF). 2016. Trends in adult body-mass index in 200 countries from 1975 to 2014: a pooled analysis of 1698 population-based measurement studies with 19.2 million participants. *Lancet*. 387:1377–1396.
- Patel M, Bernard W, Milev N, Cawthorn W, Figg N, Hart D, Prieur X, Virtue S, Hegyi K, Bonnafous S, et al. 2015. Hematopoietic IKK β limits the chronicity of inflammasome priming and metaflammation. *Proc Natl Acad Sci USA*. 112(2):506–511.
- Pejnovic NN, Pantic JM, Jovanovic IP, Radosavljevic GD, Djukic AL, Arsenijevic NN, Lukic ML. 2013. Galectin-3 is a regulator of metaflammation in adipose tissue and pancreatic islets. *Adipocyte*. 2(4):266–271.
- Peng L, Wen L, Shi Q-F, Gao F, Huang B, Meng J, Hu C-P, Wang C-M. 2020. Scutellarin ameliorates pulmonary fibrosis through inhibiting NF- κ B/NLRP3-mediated epithelial-mesenchymal transition and inflammation. *Cell Death Dis*. 11(11):978.
- Ren Z, Yang K, Zhao M, Liu W, Zhang X, Chi J, Shi Z, Zhang X, Fu Y, Liu Y, et al. 2020. Calcium-sensing receptor on neutrophil promotes myocardial apoptosis and fibrosis after acute myocardial infarction via NLRP3 inflammasome activation. *Can J Cardiol*. 36(6):893–905.
- Sandanger Ø, Ranheim T, Vinge LE, Bliksøen M, Alfsnes K, Finsen AV, Dahl CP, Askevold ET, Florholmen G, Christensen G, et al. 2013. The NLRP3 inflammasome is up-regulated in cardiac fibroblasts and mediates myocardial ischaemia-reperfusion injury. *Cardiovasc Res*. 99(1):164–174.
- Susic D, Varagic J. 2017. Obesity: a perspective from hypertension. *Med Clin North Am*. 101(1):139–157.
- Swanson KV, Deng M, Ting JP-Y. 2019. The NLRP3 inflammasome: molecular activation and regulation to therapeutics. *Nat Rev Immunol*. 19(8):477–489.
- Talman V, Ruskoaho H. 2016. Cardiac fibrosis in myocardial infarction—from repair and remodeling to regeneration. *Cell Tissue Res*. 365(3):563–581.
- Toldo S, Abbate A. 2018. The NLRP3 inflammasome in acute myocardial infarction. *Nat Rev Cardiol*. 15(4):203–214.
- van Hout GPJ, Bosch L, Ellenbroek GHJM, de Haan JJ, van Solinge WW, Cooper MA, Arslan F, de Jager SCA, Robertson AAB, Pasterkamp G, et al. 2017. The selective NLRP3-inflammasome inhibitor MCC950 reduces infarct size and preserves cardiac function in a pig model of myocardial infarction. *European Heart J*. 38:828–836.
- Wang J, Dong Z-H, Gui M-T, Yao L, Li J-H, Zhou X-J, Fu D-Y. 2019. HuoXue QianYang QuTan Recipe attenuates left ventricular hypertrophy in obese hypertensive rats by improving mitochondrial function through SIRT1/PGC-1 α deacetylation pathway. *Biosci Rep*. 39:BSR20192909.
- Wang J, Song M-Y, Lee JY, Kwon KS, Park B-H. 2015. The NLRP3 inflammasome is dispensable for ER stress-induced pancreatic β -cell damage in Akita mice. *Biochem Biophys Res Commun*. 466(3):300–305.
- Wang Y, Liu X, Shi H, Yu Y, Li M, Chen R. 2020. NLRP3 inflammasome, an immune-inflammatory target in pathogenesis and treatment of cardiovascular diseases. *Clin Transl Med*. 10(1):91–106.
- Willeford A, Suetomi T, Nickle A, Hoffman HM, Miyamoto S, Heller Brown J. 2018. CaMKII δ -mediated inflammatory gene expression and inflammasome activation in cardiomyocytes initiate inflammation and induce fibrosis. *JCI Insight*. 3(12):e97054.
- Xia Y, Sun X, Luo Y, Stary CM. 2019. Ferroptosis contributes to isoflurane neurotoxicity. *Front Mol Neurosci*. 11:486–486.
- Yang Y, Wang H, Kouadir M, Song H, Shi F. 2019. Recent advances in the mechanisms of NLRP3 inflammasome activation and its inhibitors. *Cell Death Dis*. 10(2):128.
- Yin Y, Yan Y, Jiang X, Mai J, Chen NC, Wang H, Yang XF. 2009. Inflammasomes are differentially expressed in cardiovascular and other tissues. *Int J Immunopathol Pharmacol*. 22(2):311–322.
- Zhang Y, Hou L, Tang W, Xu F, Xu R, Liu X, Liu Y, Liu J, Yi Y, Hu T, et al. 2019. High prevalence of obesity-related hypertension among adults aged 40 to 79 years in Southwest China. *Sci Rep*. 9(1):15838.
- Zhao Y, Li Q, Zhao W, Li J, Sun Y, Liu K, Liu B, Zhang N. 2015. Astragaloside IV and cycloastragenol are equally effective in inhibition of endoplasmic reticulum stress-associated TXNIP/NLRP3 inflammasome activation in the endothelium. *J Ethnopharmacol*. 169:210–218.
- Zhou X, Lu B, Fu D, Gui M, Yao L, Li J. 2020. Huoxue Qianyang decoction ameliorates cardiac remodeling in obese spontaneously hypertensive rats in association with ATF6-CHOP endoplasmic reticulum stress signaling pathway regulation. *Biomed Pharmacother*. 121:109518.